



**Modulated Fluorescence Detection with
Microelectromagnetic Traps**

Journal:	<i>Analytical Methods</i>
Manuscript ID:	AY-COM-11-2014-002828.R2
Article Type:	Communication
Date Submitted by the Author:	10-Feb-2015
Complete List of Authors:	Zakeri, Rashid; Indiana University, Chemistry Basore, Jose; Indiana University, Department of Chemistry Baker, Lane; Indiana University, Department of Chemistry;

ARTICLE

Modulated Fluorescence Detection with Microelectromagnetic Traps

Cite this: DOI: 10.1039/x0xx00000x

Rashid Zakeri, Joseph R. Basore, and Lane A. Baker^a

Received 00th January 2012,
Accepted 00th January 2012

DOI: 10.1039/x0xx00000x

www.rsc.org/

Microelectromagnetic traps (METs) were utilized to concentrate streptavidin modified magnetic particles from a microfluidic analyte stream. Particle capture was detected by bioconjugation either to biotinylated quantum dots or to DNA hybrids labeled with biotin and fluorescein. Subsequent modulation of the MET trapping field resulted in modulated fluorescence intensity at the MET. Detection of pM concentrations of streptavidin bound to magnetic particles and fM concentrations of DNA was possible through Fourier analysis of the modulated fluorescence response. This detection strategy represents a suitable approach to signal enhancement for magnetic pull-down assays and related technologies.

INTRODUCTION

Microscale sensors have garnered significant interest for bioanalytical applications in recent years.¹⁻⁹ For such devices, bioanalysis at low concentrations can prove difficult due to nonspecific adsorption that interferes with the signal of interest, particularly if the measurement occurs at a device surface.¹⁰ Chemical functionalization of surfaces is commonly employed to overcome nonspecific adsorption,^{11,12} but such nonfouling surfaces are not always effective.¹³ Methods and approaches to combat nonspecific adsorption or to differentiate between specific and nonspecific binding are thus of great interest. In this report, we utilize microcoils or straight microwires as frequency-modulated microelectromagnetic traps (METs) as a method to enhance signal-to-noise ratios and enhance differentiation from sources of background fluorescence.

Previous work by our group and others has demonstrated that METs can be utilized to manipulate magnetic particles and ferrofluids.^{14,15} For instance, use of an alternating current to move magnetic material into or out of the center of the coil-shaped MET has been demonstrated.¹⁵⁻¹⁷ Movement of particles in the vicinity of a magnetic trap relies on geometry of the microcoil and direction of current through the microcoil to control position and magnitude of the magnetic field gradient. By modulating the current, the local maxima and minima of the magnetic field can be modulated, which in turn generates a frequency dependent signal. In previous reports, we utilized electrochemical transduction, here we extend this concept to fluorescence measurements for signal enhancement of bioanalytical assays. The high affinity interaction between biotin and streptavidin was used as a model biochemical interaction to show the benefit of a modulated fluorescent signal over a static signal. Fourier transform of the fluorescence intensity in the center of the magnetic trap enhances the signal-to-noise ratio, as demonstrated in a system of magnetic particles (MPs) functionalized with streptavidin and core-shell (CdSe, ZnS) quantum dots (QDs) modified with biotin. From the information gained in these proof-of-

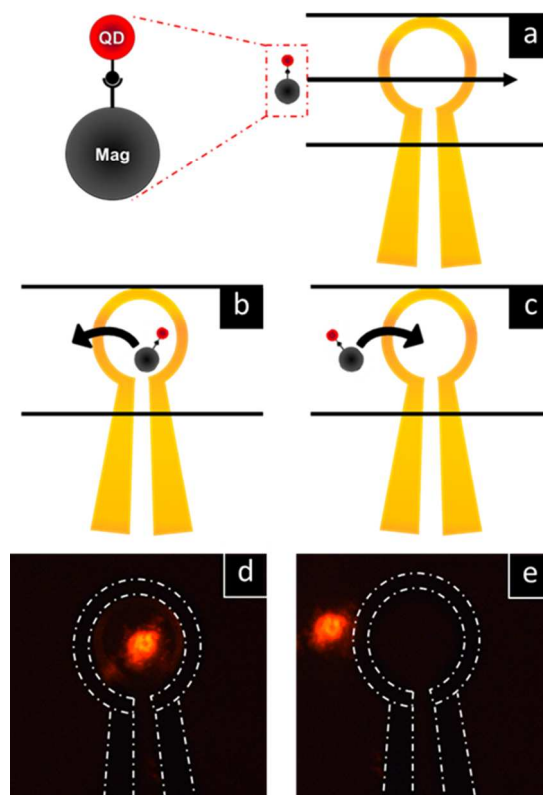


Figure 1. Scheme and optical micrographs of detection platform. (a) Illustration of bound particles driven through a microchannel over a microelectromagnetic trap (MET). (b,c) Illustration of modulation of particle position with magnetic field. (d,e) Optical fluorescence images which show the ability to control position of particles about the MET.

concept experiments, a simpler straight-wire trap was developed for detection of complementary DNA sequences.

EXPERIMENTAL SECTION

Chemicals: Magnetic microparticles functionalized with streptavidin were purchased from Invitrogen (Grand Island, NY). Core-shell QDs with carboxylic acid end groups were purchased from Ocean Nanotech (Springdale, AR). Amine terminated biotin (EZ-Link) was purchased from Thermo-Scientific (Waltham, MA). N-Hydroxysuccinamide (NHS), 1-ethyl-3-(3-dimethylaminopropyl) carbodiimide (EDC) and triton-X surfactant were purchased from Sigma-Aldrich (St. Louis, MO). Polydimethylsiloxane (PDMS) was purchased from Dow Corning (Midland, MI). Methoxy-poly(ethylene-glycol)-silane (PEG-SIL) was purchased from Laysan Bio Inc. (Arab, AL). Nuclease-free DNA buffer solution (0.010 M tris) was purchased from Integrated DNA Technologies (Coralville, Iowa). All solutions were prepared in 18 M Ω -cm deionized water from a Milli-Q purification system (EMD Millipore Corp., Billerica, MA).

Microelectromagnetic traps: Microelectromagnetic traps with coil geometries were fabricated as described previously.¹⁷ Briefly, a 3x3 array of MET chips, each with six individually addressable traps, was fabricated on Pyrex wafers. Positive tone photoresists were used to lithographically define the initial MET electrode geometry. Metal evaporation was used to deposit a conductive seed layer on the pyrex wafer. Further photolithographic methods and electrochemical deposition were utilized to create a 3-5 μ m thick Au MET with an outer ring diameter of 100 μ m. After electrode fabrication, METs were insulated with 100 nm of SiO₂ via atomic layer deposition.

Microelectromagnetic traps with straight wire geometry were fabricated with a simpler design on printed circuit boards (PCBs) (Advanced Circuits, Aurora, CO). Each chip was made with 3 parallel wires across the middle of the PCB. The width of each wire was 150 μ m, with 400 μ m space between each wire. Wires were individually connected to 5 x 5 mm contact pads and each wire had a copper core with a silver over-layer.

Particles: Streptavidin-functionalized magnetic particles (diameter = 1 μ m) were washed and magnetically separated 3 times in 0.1 M PBS buffer solution (pH = 7.4). Quantum dots with carboxylic acid surface groups were biotinylated with carbodiimide chemistry through EDC/NHS coupling.¹⁸ Prior to introduction to the MET, a range of sample concentrations were prepared by mixing an aliquot of biotinylated-QDs and a streptavidin-modified MP solution in 0.1 M PBS buffer (pH 7.4). The concentration of QDs was held constant at 40 nM while the concentration of streptavidin present on modified MPs was varied in concentration from 0.900 pM to 14.4 nM. (Concentrations as described here refer to the amount of streptavidin bound by magnetic particles.)

Single stranded target and capture DNA sequences (21 bases long) were purchased from Integrated DNA Technologies (Coralville, IA). Strands were further modified with a fluorescein terminus at the 5' end (5'-/56-FAM/CTG CAA GTC GAG TTA CGA AAC -3') of the receptor sequence and with a biotin terminus on the 5' end (5'-/Biotin/GTT TCG TAA CTC GAC TTG CAG -3') of the capture sequence. Biotinylated target DNA was first bound to the streptavidin-functionalized magnetic particles. Magnetic particles bound with DNA were then mixed with different concentrations of capture DNA, hybridized for 20 min, and tested with the MET. Solutions of 0.010 M tris-buffer were used for all DNA experiments.

Human blood was freshly drawn in 250 μ L aliquots and diluted to 1% or 5% (vol/vol) with the 0.010 M tris-buffer.

Microfluidic Channel: Figure 1a shows an illustration of particles introduced to a MET through a microfluidic channel. Channels (500 μ m width, 200 μ m height) were prepared by spin coating PDMS onto pre-fabricated silicon masters followed by curing for 1h at 110 $^{\circ}$ C.¹⁹ A thin PDMS layer was also coated onto the MET to further insulate the trap and to tune the maximum magnetic field strength at the coil center.²⁰ To bind the channel over the MET, the respective surfaces were treated in a plasma cleaner at 18 W (Harrick PDC-32G) for 3 min. The two activated surfaces were then aligned and pressed to close contact to bond the microchannel over the top of the MET. To minimize nonspecific adsorption, the channel was functionalized by passing a dilute solution (10 mM) of methoxy-poly(ethylene glycol) silane (PEG-SIL) through the channel. Additionally, in low concentration experiments, a blocking solution of bovine serum albumin (BSA) was passed through the fluidic device prior to analysis to reduce nonspecific adsorption.²¹ Solutions of fluorophores bound to MPs were passed over an energized MET for a fixed duration to concentrate the MPs at the METs. After termination of flow, the system was allowed to equilibrate for 1 minute. Direction of electric current through the MET (300 mA for coils and 1000 mA for wires) was then switched at a frequency of 33 mHz, to create a periodic shift in location of the maximum of the magnetic field gradient and subsequently move the particles about the MET. For MET-coils, particles moved in and out of the coil center (Figure 1b,c) and thus, QDs bound to MPs could be differentiated from background fluorescence. Fluorescence intensity at the MET traps was integrated with respect to time as observed by fluorescence microscopy (Nikon Eclipse E800). Fourier analysis of time-dependent data was performed via OriginPro 9.

RESULTS AND DISCUSSION

MET-coils with Biotin-Streptavidin

Microfluidic channels were used to facilitate sample introduction and to reproducibly control the amount of solution to which traps were exposed and the duration of exposure (shown schematically, Figure 1). Sample was introduced to the MET by injection of a 140 μ L aliquot of known concentration (40 nM biotin-QD, 0.900 pM – 14.4 nM streptavidin-MP) into the channel, which was then passed over the MET at a rate of 7 μ L/min. This process is shown schematically in Figure 1a-c.

A solution of magnetic particles labelled with quantum dots was passed over a MET with the coil energized to trap particles at the center. When the direction of the current was switched, particles trapped at the center of the trap moved to the periphery. Single frames of each trapping state are shown in Figure 1d,e. Aggregated QD-MPs were held at the MET center (Figure 1d). Upon reversal of the current direction, the aggregate was moved to the outside of the coil (Figure 1e).

Changes in fluorescence intensity at the center of the MET were measured as a function of time, while the current was periodically reversed. Plots of intensity recorded at the MET center as particles were moved into and out of the trap are shown in Figure 2. Higher concentrations of streptavidin (nM, bound to magnetic particles) can be measured by fluorescence intensity and can be differentiated from the background with a signal-to-noise ratio of 3.8. At picomolar

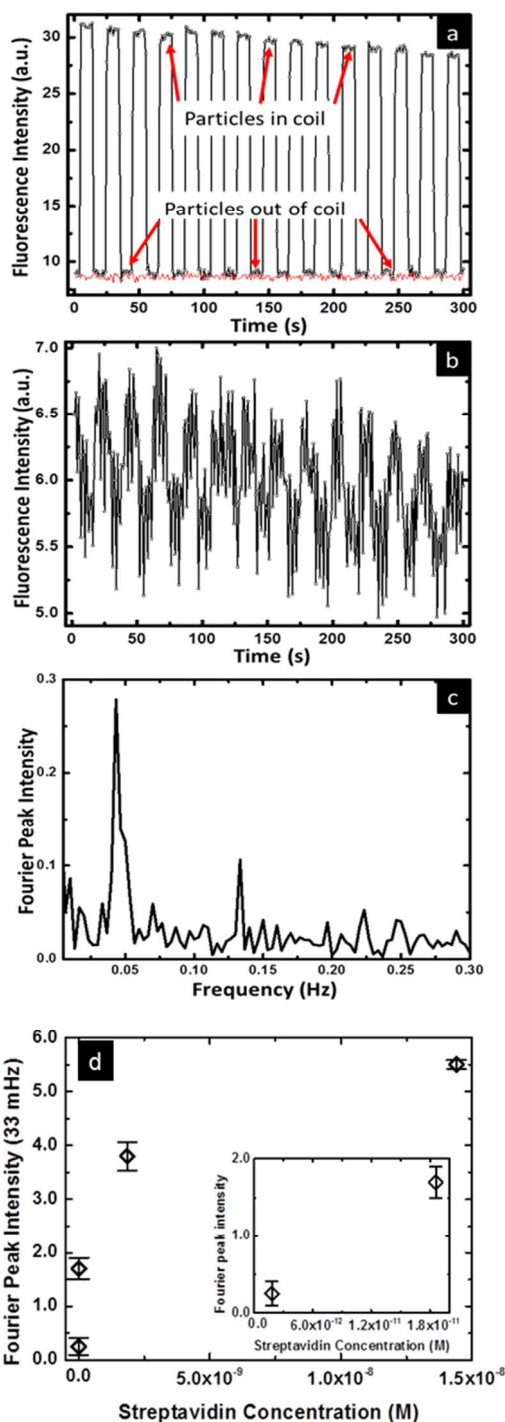


Figure 2. (a) Integrated fluorescence intensity of trapped particles after a solution of 14.4 nM streptavidin was passed over the coil. Particles were moved into and out of the coil at 33 mHz, red line is the observed baseline noise. (b) Intensity plot of a 1.84 pM streptavidin sample measured with the same conditions used in (a). (c) Fourier analysis of plot in (b). (d) Plot of Fourier peak intensity at 33 mHz as it varies with streptavidin concentration in the nM to pM range (14.4 nM, 1.86 nM, 18.6 pM, 1.84 pM). Inset: 18.6 pM and 1.84 pM concentrations. (streptavidin concentration means the amount of streptavidin bound to

concentrations, the observed signal-to-noise ratio was much lower ($S/N \sim 1.0$). Figure 2b shows fluorescence intensity measured under the same experimental conditions as Figure 2a, but with a concentration of 1.84 pM. As modulation of particle position occurred at a constant frequency, the Fourier transform (Figure 2c) of data recorded in Figure 2b could be used to provide significant enhancement in signal-to-noise ($S/N \sim 10$). Of note, the primary frequency from the Fourier analysis at low signal to noise was commonly shifted from the actual modulation frequency (In Figure 2c, 0.4 mHz vs. 0.33 mHz modulation frequency). We believe this occurs due to a combination of a lag in physical movement of particles and from operating at the edge of the signal to noise ratio, where for instance in Figure 2b, the apparent modulation time is inconsistent due to the lower signal to noise ratio. The net effect of this is that cycles appear wider and the apparent average frequency increases. This approach of position modulation with subsequent Fourier analysis affords low concentration detection not possible without modulation. When applied to a range of concentrations, as shown in Figure 2d, the amplitude of the Fourier peak intensity at the modulation frequency was used to produce a calibration curve. Under the experimental conditions used here, an upper detection limit was observed to be in the tens of nM range (max range not shown). However, this upper limit can be extended by introduction of smaller initial aliquots of sample. Likewise, lower concentrations of analyte could be detected by increasing the volume of analyte passed over the MET in the initial particle trapping period of analysis due to the inherent extraction capabilities of traps.

MET-wires with DNA

Microelectromagnetic traps with a coil geometry showed that particles could be trapped and analyzed, but MET-coils were limited due to their size (100 μm diameter) versus the width of the microfluidic channels (500 μm) (Figure 3a). This coil size limited the capture area of MPs that flowed through the channel. To increase capture efficiency, a new MET with a straight wire was developed to span the width of the channel. Either geometry, a straight microwire or a microcoil can be utilized to make a MET, but the radius of the turn in the microcoil provides a region of field enhancement, which means that microwires need higher currents to generate equivalent fields. The current magnitude required to trap the majority of particles from the microfluidic stream is also related to the channel height. In previous work, we have used finite element simulations to estimate distances the magnetic field extended from the surface.¹⁵⁻¹⁷ For microwires used here, amount of magnetic particles trapped for a range of different currents was monitored via optical microscopy, which resulted in selection of currents used here, where essentially all particles could be trapped. In a microwire MET as described here, particles concentrate on one side of the wire and when the direction of current through the wire is reversed, magnetic material moves to the opposite side of the wire. Modulating the current alternates the side of the wire the particles reside at, similar to the microcoil described above. Printed circuit boards (PCBs) were chosen as a platform for new METs due to the fact they are commercially available with wire widths and lengths that are appropriate for the size scale of the microfluidic channels.

To further illustrate the utility of METs in bioassay platforms, model complementary DNA sequences were investigated. Biotinylated primary DNA was bound to streptavidin functionalized MPs. Next, a compliment receptor DNA with a fluorescent tag was mixed with the DNA-MPs and allowed to hybridize for 20 min. In these

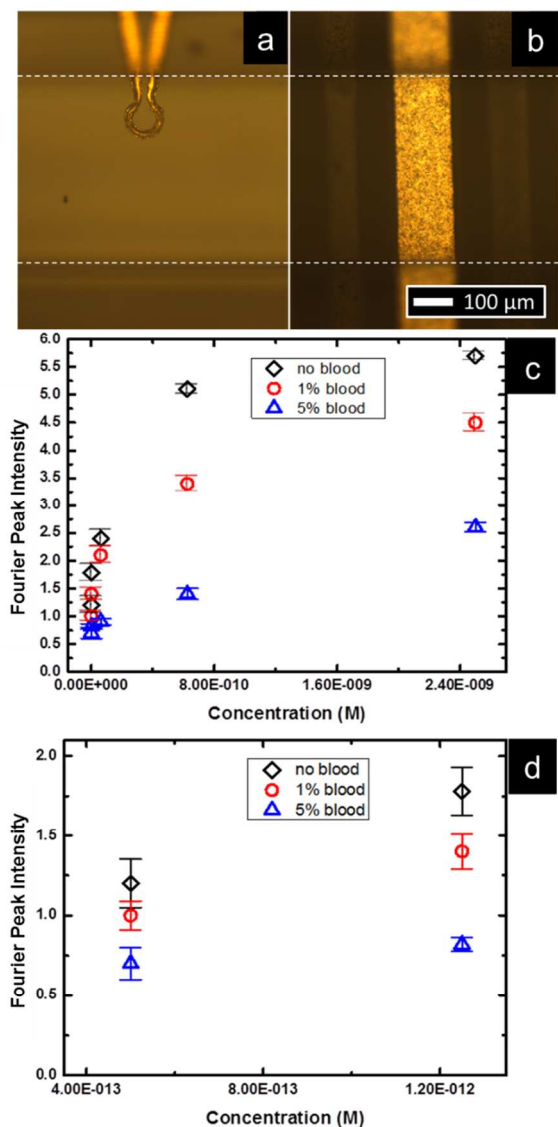


Figure 3. Optical images of two microelectromagnetic traps with PDMS microfluidic channels over them, dotted white lines highlight edges of each channel. (a) Single turn MET physically covers $\sim 20\%$ of the channel width while (b) straight wire MET provides consistent electromagnetic field across 100% of the channel width. (c and d) Plot of Fourier intensity peaks at 33 mHz of bound receptor DNA. (c) For all data primary DNA concentration was held constant at 250 nM while receptor DNA concentrations were run at 2.50 nM, 625 pM, 62.5 pM, 1.25 pM and 500 fM. Black trace illustrates samples run in 0.010 M Tris-buffer (0.050 M NaCl), while the red and blue traces represent samples with the addition of 1% and 5% blood, respectively. (d) Zoomed in plot of data for sample concentrations of 1.25 pM and 500 fM ($n \geq 4$ for all data).

experiments the concentration of MPs remained the same while the model analyte (fluorescently tagged DNA) concentrations were varied. Preliminary studies showed that a range of DNA concentrations, in tris-buffer (0.010 M), were reproducibly detected

across five orders of magnitude from 2.5 nM to 500 fM, Figure 3c (black trace). While detection of bound biomolecules is an important component, the ability to detect a target analyte in a complex matrix (blood) is a factor in bioanalysis. To determine the MET's ability to concentrate and detect bound DNA, human blood, diluted to final concentrations (volume %) of 1% or 5% were added to solution prior to DNA hybridization. As seen in Figure 3c-d, even with the addition of diluted whole blood, target DNA was still reproducibly detected at both blood concentrations. For each case in Figure 3, all sample sets follow the same trend regardless of the addition of blood. The intensity for samples with blood drops 25% and 60% respectively for 1% and 5% samples in blood. In these experiments blood represents a matrix that could interfere through nonspecific adsorption of material to the particle surface, or channel surfaces (blood does not represent a specific DNA hybridization assay of interest). These preliminary results show that particle capture, position modulation and Fourier analysis with METs provides a method that can be used to enhance the performance in a versatile manner.

CONCLUSIONS

Similar to other magnetic pull-down assays, METs provide the opportunity to concentrate magnetic material from solution as the solution is passed over the MET. However, unlike other magnetic assays, the field of a MET can be rapidly reversed by changing the current through the trap, which can be advantageous for sensor design. We have demonstrated a MET platform amenable to assays that utilize fluorescence as the analytical signal. By modulating the current through traps at a defined frequency, Fourier transform of the fluorescent intensity at a fixed location relative to the trap can be used to aid in discrimination from background fluorescence. This concept was utilized in two trap geometries, microcoil and microwire, and with two different model analyte-receptor pairs, biotin-streptavidin and hybridized DNA. This platform can easily be extended to other assays that utilize magnetic beads and provides a general route to enhance the performance of magnetic pull-down biosensors. Future directions of this work may include creating an array of wires within a channel where each wire can be used to sequester a specific population of magnetic beads labelled with one half of a sandwich assay for capture of a unique analyte. Here control of current through the wire can be used to turn capture wires on or off, in effect addressing the array. Analyte solution will be passed over the array of magnetic beads, followed by fluorescent beads labelled with the second half of each sandwich assay, which will serve to label magnetic particles at each wire. Modulating the position and Fourier analysis can then be performed by monitoring the spatial component of fluorescence at each wire as described here. In this manner, we expect a multi-analyte format with internal standards can be developed with the simple approaches described in this report.

ACKNOWLEDGMENTS

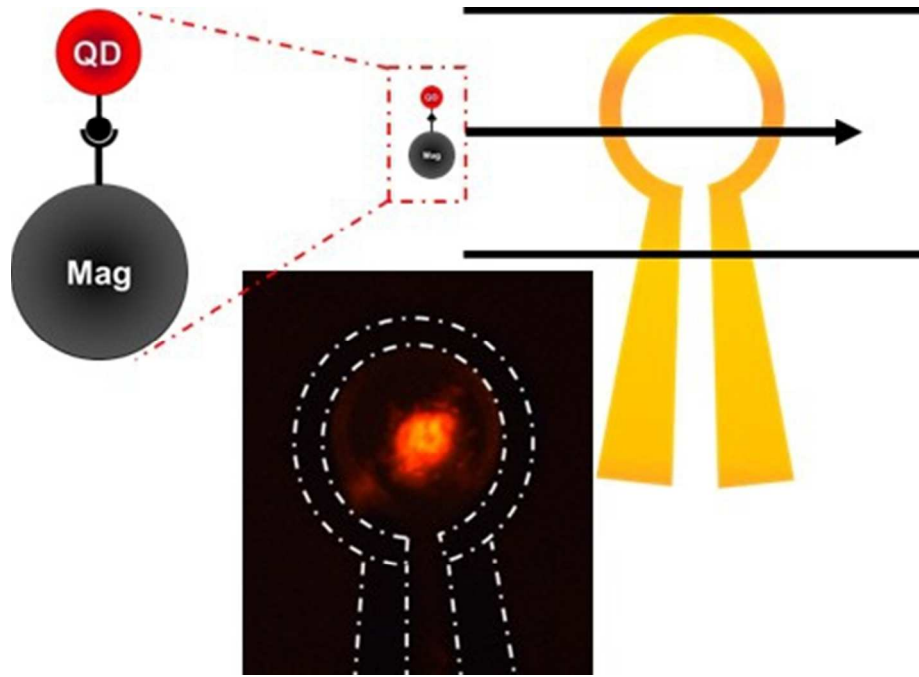
Financial support was provided by the National Science Foundation (CHE-0847624) and Oak Ridge National Laboratory - Center for Nanophase Materials Sciences (ORNL-CNMS, project # CNMS2012-219)

Notes and references

^a Department of Chemistry
Indiana University
800 E. Kirkwood Ave
Bloomington, IN 47405
USA

- 1
 - 2
 - 3
 - 4
 - 5
 - 6
 - 7
 - 8
 - 9
 - 10
 - 11
 - 12
 - 13
 - 14
 - 15
 - 16
 - 17
 - 18
 - 19
 - 20
 - 21
 - 22
 - 23
 - 24
 - 25
 - 26
 - 27
 - 28
 - 29
 - 30
 - 31
 - 32
 - 33
 - 34
 - 35
 - 36
 - 37
 - 38
 - 39
 - 40
 - 41
 - 42
 - 43
 - 44
 - 45
 - 46
 - 47
 - 48
 - 49
 - 50
 - 51
 - 52
 - 53
 - 54
 - 55
 - 56
 - 57
 - 58
 - 59
 - 60
1. T. A. Brettell, N. Rudin and R. Saferstein, *Anal. Chem.*, 2003, **75**, 2877-2890.
 2. R. Gasparac, B. J. Taft, M. A. Lapierre-Devlin, A. D. Lazareck, J. M. Xu and S. O. Kelley, *J. Am. Chem. Soc.*, 2004, **126**, 12270-12271.
 3. L. He, M. D. Musick, S. R. Nicewarner, F. G. Salinas, S. J. Benkovic, M. J. Natan and C. D. Keating, *J. Am. Chem. Soc.*, 2000, **122**, 9071-9077.
 4. S. Husale, H. H. J. Persson and O. Sahin, *Nature*, 2009, **462**, 1075-1078.
 5. C. S. Liao, G. B. Lee, J. J. Wu, C. C. Chang, T. M. Hsieh, F. C. Huang and C. H. Luo, *Biosens. Bioelectron.*, 2005, **20**, 1341-1348.
 6. J. M. Nam, S. I. Stoeva and C. A. Mirkin, *J. Am. Chem. Soc.*, 2004, **126**, 5932-5933.
 7. L. L. Pang, J. S. Li, J. H. Jiang, Y. Le, G. L. Shen and R. Yu, *Sens. Actuators, B*, 2007, **127**, 311-316.
 8. M. Passamano and M. Pighini, *Sens. Actuators, B*, 2006, **118**, 177-181.
 9. K. Feng, J. Li, J. H. Jiang, G. L. Shen and R. Q. Yu, *Biosens. Bioelectron.*, 2007, **22**, 1651-1657.
 10. V. Sharma, M. Dhayal, Govind, S. M. Shivaprasad and S. C. Jain, *Vacuum*, 2007, **81**, 1094-1100.
 11. J. Zhou, A. V. Ellis and N. H. Voelcker, *Electrophoresis*, 2010, **31**, 2-16.
 12. J. Zhou, D. A. Khodakov, A. V. Ellis and N. H. Voelcker, *Electrophoresis*, 2012, **33**, 89-104.
 13. K. L. Brogan, J. H. Shin and M. H. Schoenfish, *Langmuir*, 2004, **20**, 9729-9735.
 14. J. Basore and L. Baker, *Anal. Bioanal. Chem.*, 2012, **403**, 2077-2088.
 15. J. R. Basore, N. V. Lavrik and L. A. Baker, *Chem. Commun.*, 2012, **48**, 1009-1011.
 16. J. R. Basore, N. V. Lavrik and L. A. Baker, *Adv. Mater.*, 2010, **22**, 2759-2769.
 17. J. R. Basore, N. V. Lavrik and L. A. Baker, *Langmuir*, 2010, **26**, 19239-19244.
 18. Z. Grabarek and J. Gergely, *Anal. Biochem.*, 1990, **185**, 131-135.
 19. J. C. McDonald, D. C. Duffy, J. R. Anderson, D. T. Chiu, H. Wu, O. J. A. Schueller and G. M. Whitesides, *Electrophoresis*, 2000, **21**, 27-40.
 20. H. Lee, A. M. Purdon and R. M. Westervelt, *IEEE Trans. Magn.*, 2004, **40**, 2991-2993.
 21. N. C. H. Le, V. Gubala, R. P. Gandhiraman, S. Daniels and D. E. Williams, *Langmuir*, 2011, **27**, 9043-9051.

1
2
3
4
5
6
7
8
9
10
11
12
13
14
15
16
17
18
19
20
21
22
23
24
25
26
27
28
29
30
31
32
33
34
35
36
37
38
39
40
41
42
43
44
45
46
47
48
49
50
51
52
53
54
55
56
57
58
59
60



77x56mm (150 x 150 DPI)